Preprints, 10th IFAC International Symposium on
Advanced Control of Chemical Processes
Shenyang, Liaoning, China, July 25-27, 2018

Extraction of Plant-wide Oscillations using Fast Multivariate Empirical Mode Decomposition ⋆

Xun Lang * **Zhiming Zhang** * **Qian Zheng** * **Lei Xie** *
Alexander Horch ** **Hongye Su** *

* *State Key Laboratory of Industrial Control Technology, Zhejiang University, 310027 Hangzhou, China (e-mail: langxun@zju.edu.cn (Xun Lang), leix@iipc.zju.edu.cn (Lei Xie)).*
** *HIMA Paul Hildebrandt GmbH, Albert-Bassermann-Str. 28, 68782 Bruehl bei Mannheim, Germany (e-mail: a.horch@hima.com)*

Abstract: This paper proposes a novel time-frequency method for plant-wide oscillation analysis based on the multivariate extension of standard empirical mode decomposition (EMD). The raised fast multivariate empirical mode decomposition (FMEMD) is generalized from EMD by solving an overdetermined system of linear equations. Due to its capability to analyze multiple channels data, FMEMD is especially suitable for characterizing plant-wide control loop oscillations. Unlike traditional methods, both the regularity of oscillations (in frequency domain) and evolution of local characteristics (in time scale) can be well captured via FMEMD. Validity of the raised approach is demonstrated on simulations as well as an industrial case.

Keywords: EMD, FMEMD, plant-wide oscillations, overdetermined linear equations.

1. INTRODUCTION

Plant-wide oscillation detection and characterization is one of the important issues in many process industries (Thornhill et al. (2003a)). The presence of oscillatory variables in a process plant may result in inferior products, larger rejection rates, and even compromise process stability (Thornhill et al. (2002)). Therefore, it is important and challenging to automatically detect such oscillations in order to maintain efficient operation.

Existing oscillation detecting methods can be roughly divided into univariate and multivariate ones, while most of these techniques are designed for being applying to single time series (Lang et al. (2018)). With respect to multivariate techniques, Thornhill et al. (2002) proposed the spectral principal component analysis (SPCA) to detect and categorize the variables having similar oscillations. In 2005, a new visualization tool termed as power spectral correlation map (PSCMAP) is raised by Tangirala et al. (2005). More recently, Jiang et al. (2007) presented the spectral envelope method for detection and diagnosis of plant-wide oscillation, and El-Ferik et al. (2012) proposed the spectral decomposition based on evolutionary algorithm. However, there are some crucial restrictions of Fourier spectral analysis: the system must be linear, and the data must be strictly periodic or stationary.

⋆ The authors would like to thank sponsor and financial support from Natural Science Foundation of Zhejiang, China (No. LR17F030002), Science Fund for Creative Research Groups of the National Natural Science Foundation of China (No.61621002) and China MIIT Project: Research on the standard of software interoperability interface specification between ERP/MES and control system and the construction of testing/verification platform.

Recently, multivariate EMD (MEMD), was introduced by Rehman and Mandic (2009). MEMD allows simultaneous processing of multi-dimensional signals that are composed of data collected from different control loops. This algorithm has all the advantages of standard EMD (Huang et al. (1998)) in analyzing nonlinear and nonstationary time series, and additionally can align the common intrinsic mode functions (IMFs). However, it seems a common belief that a major drawback of the MEMD is that it requires a long computation time (Wu et al. (2010)). Moreover, according to Rehman and Mandic (2009), the sifting for a multivariate IMF can only be stopped until all the projected signals fulfill the stoppage criteria. Notice that enforcing the same number of siftings for every data channel will inevitably induce the affect of over-decomposition and compromise the time-frequency information further.

To resolve the issues above, a novel multivariate extension of EMD, namely FMEMD, is proposed in this study. The standard EMD is first applied on the projected signals to extract a set of univariate IMFs, the combination of such IMFs is then solved by the least square algorithm to yield the desired multivariate IMF. Running of FMEMD is at least p times faster than the existing MEMD, and in addition, avoid the ambiguities of notion on multivariate sifting. When analyzing on white Gaussian noise, FMEMD also outperforms MEMD in responding as a dyadic filter bank on each dimension of the multivariate signal.

The rest of this paper is organized as follows. The EMD and MEMD are first reviewed in Section 2, additionally, Section 3 addresses the proposed fast MEMD method. The simulation based analyses of FMEMD versus MEMD are presented in Section 4. Section 5 discusses an industrial case, which is followed by conclusions in Section 6.

2. PRELIMINARIES

2.1 Empirical mode decomposition

The standard EMD aims to adaptively decompose a signal into a finite set of oscillatory components known as intrinsic mode functions (IMFs) (Huang et al. (1998)). More specifically, for a real valued signal $x(t)$, the application of EMD yields M sets of IMFs, denoted as $\{d_i(t)\}_{i=1}^{M}$, and a monotonic residue $r(t)$, so that

$$x(t) = \sum_{i=1}^{M} d_i(t) + r(t) \tag{1}$$

where the residual signal $r(t)$ is a monotonous function. The procedures used for extraction of IMFs from a real-valued signal $x(t)$ are summarized in Algo. 1.

Algorithm 1 Empirical mode decomposition.

Input: $x^1(t) = x^2(t) = x(t)$, $i = 1$

1: Find the locations of all the extrema of $x^1(t)$;
2: Interpolate all the maxima (minima) to obtain the upper (lower) envelop, $e_{\max}(t)$ ($e_{\min}(t)$);
3: Find the local mean, $m(t) = [e_{\min}(t) + e_{\max}(t)]/2$;
4: Subtract the mean from the signal to obtain an oscillatory mode, $s(t) = x^1(t) - m(t)$;
5: If $s(t)$ obeys the stoppage criteria, $d_i(t) = s(t)$ becomes an IMF, go to step 6. Otherwise set $x^1(t) = s(t)$ and repeat the process from step 1;
6: Subtract the so derived IMF from $x^2(t)$, so that $x^2(t) := x^2(t) - d_i(t)$. If $x^2(t)$ becomes a monotonic function, stop the sifting process with $r(t) = x^2(t)$. Otherwise, $x^1(t) = x^2(t)$, $i = i + 1$ and go to step 1;
7: **return** $\{d_i(t)\}_{i=1}^{M}$ and $r(t)$;

2.2 Multivariate Empirical Mode Decomposition

For multivariate signals, multiple p-dimensional envelopes are generated by taking signal projections along different directions in p-dimensional space, and subsequently interpolating their extrema (Rehman and Mandic (2009)). These envelopes are then averaged to obtain the local multivariate mean. Similar to standard EMD, the MEMD uses a vector-valued form of standard EMD to decompose a p-variate signal $\mathbf{x}(t)$ as

$$\mathbf{x}(t) = \sum_{i=1}^{M} \mathbf{d}_i(t) + \mathbf{r}(t) \tag{2}$$

where the p-variate IMFs, $\{\mathbf{d}_i(t)\}_{i=1}^{M}$, contain scale-aligned intrinsic joint rotational modes.

3. FAST MULTIVARIATE EMPIRICAL MODE DECOMPOSITION

This section proposes a novel multivariate generalization of EMD. The main content of this section includes: (i) the extension principle from EMD to FMEMD, (ii) the specific algorithm of FMEMD and (iii) some supplementary statements.

3.1 Extension principle for FMEMD

The multi-dimensional local mean of the existed MEMD is computed as the average of multiple envelopes obtained by interpolating extrema that are extracted from the multiple projections. In practice, this method is hindered by

- *High computational cost*: The computation time of MEMD multiplied significantly as the dimension of the signal increases.
- *Over-decomposition*: Enforcing the same number of iterations for every data channel during the sifting process may compromise the extraction of IMFs.

Considering the obstacles above, a new multivariate EMD that is out of the framework of the original MEMD is required. However, in a strict sense, all forms of the multivariate generalizations are able to be considered as MEMD, if such algorithms can be simplified to the standard EMD. In order to ensure the physical meaning of the unknown multivariate IMF, the expected MEMD (namely, FMEMD) is extended underlying the basic principles of EMD and MEMD.

As an adaptive method of decomposing local temporal characteristics, the intrinsic principle that underpins EMD is to formalize the following idea (Mandic et al. (2013)):

Principle 1: EMD: univariate signal = slower oscillations + fast oscillation.

For multivariate data, similarly, the principle of separating oscillations can be generalized to that of splitting rotations (Rehman and Mandic (2009)), whereby

Principle 2: The expected MEMD: multivariate signal = slower rotations + fast rotation.

The notion of rotation, which, moreover, is arguably a multiple-dimensional extension of the usual notion of univariate oscillation (Mandic et al. (2013)), can be briefly summarized as a multivariate monocomponent that shows the aligned frequency subbands across distinct channels. Accordingly, a rotation is equal to a multivariate IMF (MIMF) in this study. Let $\mathcal{S}\mathbf{x}(t)$ denotes the first multivariate mean (slower rotations) of the input signal $\mathbf{x}(t)$, $x^{\theta_k}(t)$ represents the projection of $\mathbf{x}(t)$ along $\mathbf{v}^{\theta_k}$, and $\mathcal{S}x^{\theta_k}(t)$ denotes the first univariate mean (slower oscillations) of $x^{\theta_k}(t)$, the solution for defining a multivariate IMF is investigated:

i) According to *Principle 2*, the fast rotation (the first MIMF with the highest frequency) of the original signal, $\mathbf{x}^{fast}(t)$, is extracted preferentially, which yields the formula of $\mathcal{S}\mathbf{x}(t)$ as

$$\mathcal{S}\mathbf{x}(t) = \mathbf{x}(t) - \mathbf{x}^{fast}(t) \tag{3}$$

ii) Similarly, the fast oscillation $x^{fast}(t)$ is separated from $x^{\theta_k}(t)$ based on *Principle 1*. Subtracting $x^{fast}(t)$ from the projected function gives

$$\mathcal{S}x^{\theta_k}(t) = x^{\theta_k}(t) - x^{fast}(t) \tag{4}$$

iii) The projection of the multivariate signal $\mathbf{x}(t)$ under projection vector $\mathbf{v}^{\theta_k}$ is essentially the summation of terms that are equal to each dimension of $\mathbf{x}(t)$ multiplied by the corresponding coefficients in $\mathbf{v}^{\theta_k}$. Therefore, the projection operator only changes the amplitude of each division of

$\mathbf{x}(t)$ (the original amplitude multiplying with its corresponding coefficient), while the frequency characteristic remains. Consequently, the projection of the fast rotation $\mathbf{x}^{fast}(t)$ along vector $\mathbf{v}^{\theta_k}$ will still represent the fast oscillation in the projected function $x^{\theta_k}(t)$. From step ii), the separated fast oscillation is known as $x^{fast}(t)$, so it is concluded that

$$x^{fast}(t) = \mathbf{x}^{fast}(t) \cdot \mathbf{v}^{\theta_k} \tag{5}$$

iv) Combining Eq. 5 with the prerequisite $x^{\theta_k}(t) = \mathbf{x}(t) \cdot \mathbf{v}^{\theta_k}$, a new equation is given below

$$x^{\theta_k}(t) - x^{fast}(t) = \left[\mathbf{x}(t) - \mathbf{x}^{fast}(t)\right] \cdot \mathbf{v}^{\theta_k} \tag{6}$$

Finally the relationship between $\mathcal{S}x^{\theta_k}(t)$ and $\mathcal{S}\mathbf{x}(t)$ is deducted by integrating Eqs. 3, 4 and 6, which yields

$$\mathcal{S}x^{\theta_k}(t) = \mathcal{S}\mathbf{x}(t) \cdot \mathbf{v}^{\theta_k} \tag{7}$$

According to the analysis above, it can be concluded that,

Axiom 1. Given a specified direction vector, the projection of a multivariate mean is equal to the univariate mean that is extracted from the projected signal.

If a p-variate signal $\mathbf{x}(t)$ is projected into K directions [1], $\left\{\mathbf{v}^{\theta_k}\right\}_{k=1}^{K}$, to yield K projections, $\left\{x^{\theta_k}(t)\right\}_{k=1}^{K}$, an overdetermined linear equation set is obtained based on the proposed theorem after the univariate mean $\left\{\mathcal{S}x^{\theta_k}(t)\right\}_{k=1}^{K}$ being extracted.

$$\left\{\mathcal{S}x^{\theta_k}(t)\right\}_{k=1}^{K} = \mathcal{S}\mathbf{x}(t) \cdot \left\{\mathbf{v}^{\theta_k}\right\}_{k=1}^{K} \tag{8}$$

Accordingly, the multivariate mean of $\mathbf{x}(n)$ can be computed by solving the above equations, and the first multivariate IMF, $\mathcal{F}\mathbf{x}(t)$, is therefore subtracted into

$$\mathcal{F}\mathbf{x}(t) = \mathbf{x}(t) - \mathcal{S}\mathbf{x}(t) \tag{9}$$

The procedures above can be re-applied by setting the mean signal as a new input, then the iteration continues until a monotonic mean (trend) is obtained. In consequence, an indirect multivariate extension of the standard EMD (namely, FMEMD) is accomplished.

3.2 Algorithm of FMEMD

The aforementioned axiom enables FMEMD to be generalized indirectly by back-projecting the decomposed results of standard EMD. Based on solving an overdetermined system of linear equations which is consists of the extracted univariate means from all of the projected functions, the p-variate mean of the input data can be simply computed.

Consider a sequence of p-dimensional vectors $\mathbf{x}(t) = [x_1(t), x_2(t), \ldots, x_p(t)]$ which represents a multivariate signal with p components, and $\mathbf{v}^{\theta_k} = \left[v_1^k, v_2^k, \ldots, v_p^k\right]^T$ denoting a set of vectors along the directions given by angles $\theta_k = \left[\theta_k^1, \theta_k^2, \ldots, \theta_k^{p-1}\right]^T$ on a $(p-1)$-sphere, the proposed FMEMD is summarized in Algo. 2.

In consequence, the FMEMD uses the presented procedures to decompose a p-variate signal $\mathbf{x}(t)$ into

$$\mathbf{x}(t) = \sum_{i=1}^{M} \mathbf{d}_i(t) + \mathbf{r}(t) \tag{10}$$

Algorithm 2 Algorithm of FMEMD.

Input: $\mathbf{x^1}(t) = \mathbf{x}(t)$, $i = 1$

1: Generate a suitable point set for uniform projection;
2: Calculate the kth projection $p^{\theta_k}(t)$ of the input signal $\mathbf{x^1}(t)$ along direction vector $\mathbf{v}^{\theta_k}$, for all k (i.e. $k = 1, 2, \ldots, K$);
3: Extract univariate mean $\mathcal{S}p^{\theta_k}(t)$ of the projected function $p^{\theta_k}(t)$ for all k using standard EMD;
4: Combine the means $\left\{\mathcal{S}p^{\theta_k}(t)\right\}_{k=1}^{K}$ with their corresponding direction vectors $\left\{\mathbf{v}^{\theta_k}\right\}_{k=1}^{K}$, then the p-variate mean $\mathcal{S}\mathbf{x^1}(n)$ can be obtained by solving the following overdetermined equations

$$\left\{\mathcal{S}p^{\theta_k}(t)\right\}_{k=1}^{K} = \mathcal{S}\mathbf{x^1}(t) \cdot \left\{\mathbf{v}^{\theta_k}\right\}_{k=1}^{K} \tag{11}$$

5: The multivariate IMF is calculated by subtracting the multivariate mean from the current input signal $\mathbf{d}_i(t) = \mathbf{x^1}(t) - \mathcal{S}\mathbf{x^1}(t)$;
6: If $\mathcal{S}\mathbf{x^1}(t)$ becomes monotonous, stop the iterative process and obtain the trend, $\mathbf{r}(t) = \mathcal{S}\mathbf{x^1}(t)$. Otherwise, update the current input as $\mathbf{x^1}(t) = \mathcal{S}\mathbf{x^1}(t)$ and $i = i + 1$, then go to step 2;
7: **return** $\{\mathbf{d}_i(t)\}_{i=1}^{M}$ and $\mathbf{r}(t)$;

Remarks:

(1) In this work, the Halton and Hammersley sequence (Niederreiter (1992)) which is proven to yield improved generalized discrepancy estimates as compared with other sampling methods, is introduced for generating direction vectors.
(2) The standard EMD is a special form of the proposed FMEMD algorithm. FMEMD will be simplified to EMD when the direction vector is set to $[1]^T$.
(3) The decomposition of a multivariate signal via FMEMD exhibits mode alignment property, whereby common frequency modes in different dimensional components are aligned in a single MIMF. This property is further demonstrated in Section 5.

3.3 Solution to overdetermined equations.

To enhance the reconstruction of the multivariate mean, while attenuate some unexpected noise, the number of projections, K is usually chosen greater than the dimension of the input [2], p. As a result, Eq. 11 is usually designed into an overdetermined system of linear equations. For convenience, this system is rewritten into the form of $\mathbf{y} = \mathbf{S}\mathbf{x}$, where matrix $\mathbf{S} \in R^{K \times p}$ and vector $\mathbf{y} \in R^{K \times 1}$ are given while the vector $\mathbf{x} \in R^{p \times 1}$ is unknown. In many industrial applications, the overdetermined system is usually inconsistent, thus it is desired to find a best approximation. The well known approach (Cadzow (2002)) is to find a selection of vector $\mathbf{x}^o$ so that the ℓ_2 norm (sum of squared errors criterion) of the residual error vector

$$\mathbf{e} = \mathbf{y} - \mathbf{S}\mathbf{x}^o \tag{12}$$

is minimized. One of the main benefits accrued in employing a minimum ℓ_2 norm criterion is the existence of a closed form solution to this approximation problem. According to

[1] $K \geq p$, and it is generally set as $K > p$ for reducing noise.
[2] $K \geq 6p$ is adopted in this work.

the second theorem presented in Cadzow (2002), if matrix $\mathbf{S}$ has full column rank, there exists a unique solution to the normal equations as given by

$$\mathbf{x}^o = \left[\mathbf{S}^T\mathbf{S}\right]^{-1}\mathbf{S}^T\mathbf{y} \tag{13}$$

where $\mathbf{x}^o$ is the unique optimal solution to $\mathbf{x}$. Consequently, the optimal approximation of p-variate mean $\mathcal{S}\mathbf{x^1}(t)$ in Eq. 11 can be well captured by Eq. 13.

4. COMPARATIVE STUDY

This section compares the decomposition performance of MEMD with our proposed FMEMD. For both MEMD and FMEMD, the low-discrepancy sequences are used for generating a set of $K = 64$ direction vectors. Furthermore, end effects of the original signal were restrained in advance before MEMD/FMEMD being applied.

4.1 Computational cost.

It has been claimed in the first section that the MEMD method is computation extensive. In this section, a simple comparison between the computational load of MEMD and FMEMD is presented. It is noteworthy that some other fixed-point arithmetic operations are negligible compared with the sifting procedure [3]. Therefore, to facilitate the analysis, the sifting time based comparison is deducted between MEMD and FMEMD.

Suppose a single operation of the univariate sifting process for standard EMD requires T_0 time. According to Rehman and Mandic (2009), the multivariate envelope associated with a specified projection is computed by applying the univariate cubic spline interpolation channel-wise. Consequently, focus on each of the direction vectors, the sifting time of MEMD of a p-variate input is p times of the univariate sifting time, T_0. If totally K direction vectors are considered, the time cost of MEMD for extracting a single MIMF is given

$$T_m = n_m \cdot p \cdot K \cdot T_0 \tag{14}$$

where T_m denotes the computation cost, and n_m is the number of sifting times consumed for one MIMF extraction. In contrast to MEMD, the p-variate input of FMEMD is projected and then operated univariable using standard EMD. Therefore, the total consumption of FMEMD for a p-variate IMF computation only involves

$$T_f = \bar{n}_f \cdot K \cdot T_0 \tag{15}$$

time, where T_f denotes the time cost, while $\bar{n}_f$ represents an average of the sifting times, namely, $\bar{n}_f = \frac{1}{K}\sum_{i=1}^{K} n_i$ and n_i, $i = 1, 2, \ldots, K$ denotes the respective sifting times of standard EMD corresponding to each of the projected functions. As discussed in Rehman and Mandic (2009), the stoppage criterion for multivariate IMFs is similar to that applied for standard IMF, thus it is concluded that $n_m = \max\{n_i, i = 1, 2, \ldots, K\}$. Combine Eq. 14 with Eq. 15, a new formulation is given

$$T_m \geq p \cdot T_f \tag{16}$$

This inequality illustrates that running of the proposed FMEMD is p times or more faster than that of MEMD.

4.2 Phenomenon of over-decomposition.

In order to demonstrate that FMEMD outperforms MEMD in multivariate signal decomposition, the frequency responses and corresponding filter bank properties of MEMD and FMEMD are studied.

At first, the MEMD is applied on $N = 500$ realizations of four-channel white Gaussian noise with each of length $T = 1000$. The power spectra of the first eight MIMFs are then computed and ensemble averaged to yield an averaged power spectra as shown in the top of Fig. 1(a). It seems that MEMD is able to properly align the bandpass filters associated with the corresponding IMFs for different noise channels. However, MEMD fails to provide its frequency responses similar to that of a dyadic filter bank [4]. More specifically, zero crossings in these IMFs can not follow the structure of a dyadic filter, which shows linear (slope close to -1) relationship between the base-2 logarithm of number of zero crossings and the IMF index. The uneven blue-points in the bottom of Fig. 1(a) (with slope around -0.7409) have confirmed the statement, and further indicated that over-decomposition is inevitable when applying MEMD.

Next, the same experiment is processed based on the proposed FMEMD. Fig. 1(b) gives the averaged spectra (top) and fitting results using the base-2 logarithm of number of the zero crossings against the IMF index (bottom). It is evident from the figure that the alignment of IMF based frequency bands, in case of FMEMD, results in the stabilization of the filter bank structure. It revealed similar behavior to those obtained from standard EMD, with the slope of approximately -1.0104 for all the four channels individually, indicating a quasi-dyadic filter bank nature of FMEMD for white Gaussian noise. This noise-based simulation has well verified the superiority of FMEMD over the existing MEMD.

5. INDUSTRIAL CASE STUDY

A typical industrial case is presented in this section to demonstrate the effectiveness of the proposed method for plant-wide oscillations characterization. The data set under study is borrowed from Thornhill et al. (2003a), which is provided by a plant of Eastman Chemical Company. The uncompressed nonlinear and nonstationary plant data were sampled from the control system every 20 seconds on each of the indicators. In order to facilitate the results for displaying and analyzing, only the last 10 Tags (Tag 21 to 30) from total thirty loops with 2000 samples are investigated in this study. The decomposition results obtained by

[3] The sifting process includes all of the large computational operations, such as extrema identification and cubic spline procedures, while the rest of MEMD/FMEMD only involves some simple operations like addition, multiplication, division and an infrequent matrix operations (solving of the overdetermined system of linear equations using least squares solution).

[4] By analyzing the behavior of EMD in the presence of white Gaussian noise, Flandrin et al. (2004) shows that standard EMD essentially acts as a dyadic filter bank. Similarly, as a generalized form of EMD, MEMD should also follow this filter bank structure.

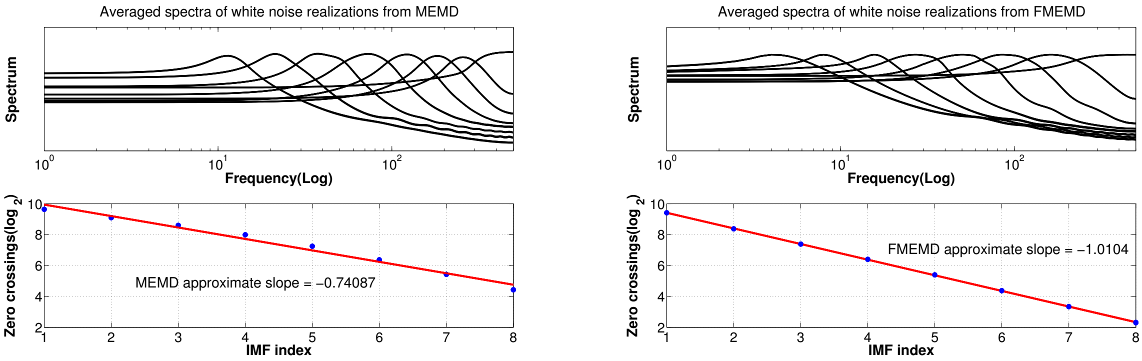

(a)

(b)

Fig. 1. Top: averaged spectra of IMFs (IMF1-IMF8) obtained from a $N = 500$ realizations of four-channel white Gaussian noise by (a) MEMD, and (b) FMEMD. Bottom: averaged number of base-2 logarithm of zero crossings plotted versus the IMF index (a) MEMD, and (b) FMEMD.

FMEMD are presented in Fig. 2. For simplicity, the first five adjacent IMFs are added together. The top row of Fig. 2 gives the process output, and the second and third rows are $\mathbf{d_1} - \mathbf{d_5}$ and $\mathbf{d_6}$ respectively. The fourth row ($\mathbf{d_7}$) denotes the plant-wide oscillations. $\mathbf{d_8}$ is shown in the fifth row and last row ($\mathbf{r}$) is the remainder of the process data.

Generally, an oscillation is considered to be regular if the standard deviation σ_T of its zero-crossing intervals T_i is less than one third of the mean value μ_T (Thornhill et al. (2003b)). Therefore, the oscillation detection index z proposed by Thornhill et al. (2003b) is adopted in this work for monitoring the decomposed rotations. This regularity index is defined as

$$z = \frac{1}{3} \times \frac{\mu_T}{\sigma_T} \tag{17}$$

which measures the variability relative to the mean. A signal is concluded to be oscillatory if its coefficient variable satisfies $z > 1$.

Table. 1 depicts the monitoring results of $\mathbf{d_6}$ and $\mathbf{d_7}$, respectively. $\mathbf{d_8}$ is not taken into account since none of the significant components exists in this scale. Obviously, an unignorable plant-wide oscillation is correctly detected in rotation $\mathbf{d_7}$. Several tags (22 to 29) shows greatly indexes in comparison with the confidence limit ($z > 1$), while only two of the loops can not detect obvious oscillation. A reasonable explanation is that Tag 21 is dominated by the nonstationary trend, and Tag 30 is caught into some intensive noise. In addition, combining Table. 1 with the time-frequency characteristics of these rotations shows that a slow plant-wide oscillation with a period around 115 min is presented throughout this plant. The interpretation in (Thornhill et al. (2003a)) that it is a prominent and widespread disturbance that accounts for most of the process variability, further confirms the detecting results accomplished by FMEMD. Compared with traditional methods (such as spectral PCA and spectral envelop), the proposed FMEMD shows several advantages from the following:

(1) time-frequency information: FMEMD can not only preserve the regularity of oscillations, but also precisely capture the critical evolution of the oscillatory components in time scale.
(2) processing nonstationarity: FMEMD is especially suitable for extraction and isolation of the nonstationary trends, as depicted in the last row of Fig. 2.
(3) adaptivity: unlike the Fourier-based approaches that employ predefined basis functions, the FMEMD is applied locally and adaptively.

Finally, a table (Table. 2) that compares the main differences and similarities between FMEMD/EMD and other standard methods is added, enabling readers to keep an overview of popular methods for time-frequency analysis.

6. CONCLUSION

A novel extension of standard EMD to FMEMD has been provided to extract the p-variate common oscillations from multiple control loops.

The mode-aligned property of FMEMD contributes to the automatic categorizing of the same frequency oscillations as well as providing both time and frequency scales information. Compared with the MEMD, the proposed approach ensures the processing of multivariate data with less computational cost and fewer IMF groups. FMEMD also outperforms traditional methods in nonlinear and nonstationary data analysis.

Simulations and an industrial case have verified the effectiveness of the method in analyzing noise-contaminated plant-wide oscillations. Future works will focus on source localization of the oscillations based on FMEMD.

ACKNOWLEDGEMENTS

The authors gratefully acknowledge the industrial data supporting from the group of Nina F. Thronhill.

REFERENCES

Cadzow, J.A. (2002). Minimum 1, 2, and infinite norm approximate solutions to an overdetermined system of linear equations. *Digital Signal Processing*, 12(4), 524–560.

El-Ferik, S., Shareef, M.N., and Ettaleb, L. (2012). Detection and diagnosis of plant-wide oscillations using ga based factorization. *Journal of Process Control*, 22(1), 321–329.

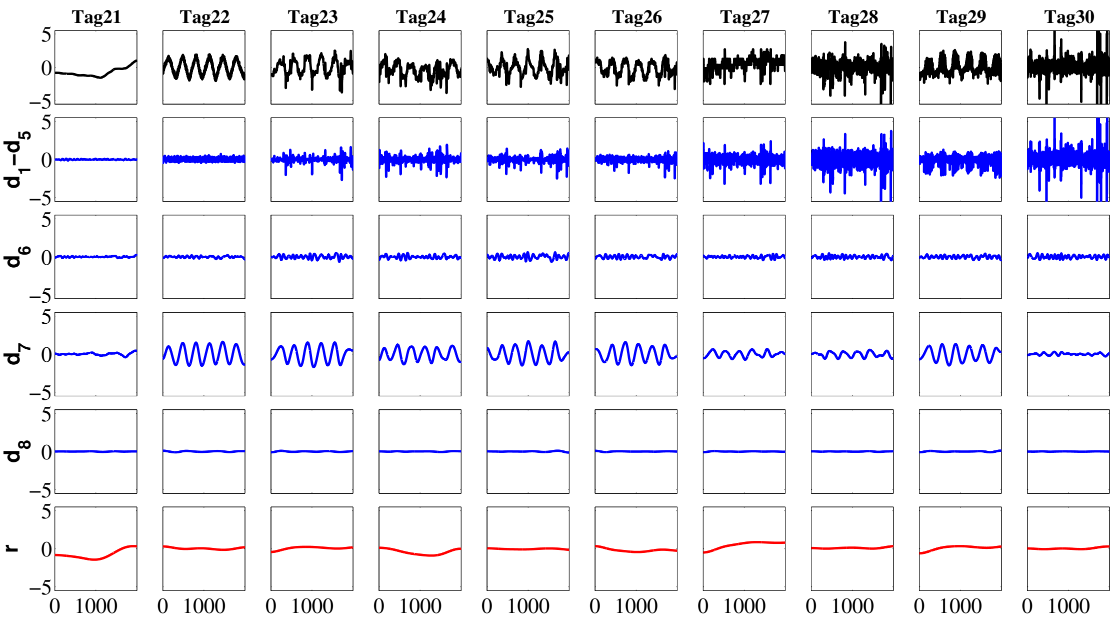

Fig. 2. Decomposition results of the process outputs using FMEMD.

Table 1. Oscillation indexes of the decomposed rotations.

Variable	Tag 21	Tag 22	Tag 23	Tag 24	Tag 25	Tag 26	Tag 27	Tag 28	Tag 29	Tag 30
$\mathbf{d}_6$	0.3636	0.5686	0.8246	0.8074	0.7499	0.6354	0.5218	0.6373	0.9437	0.6667
$\mathbf{d}_7$	0.6114	2.9346	3.0956	3.0562	2.6970	3.0569	1.7429	1.3659	3.0348	1.0786

Table 2. Comparison of the main methods for time-frequency (TF) analysis.

Methods	TF information	Adaptive	Nonlinear	Nonstationary	Mode-alignment	Reversible
Fourier	No	No	No	No	No	Yes
Wavelet	Yes	No	No	Yes	No	Yes
EMD	Yes	Yes	Yes	Yes	No	No
FMEMD	Yes	Yes	Yes	Yes	Yes	No

Flandrin, P., Rilling, G., and Goncalves, P. (2004). Empirical mode decomposition as a filter bank. *IEEE signal processing letters*, 11(2), 112–114.

Huang, N.E., Shen, Z., Long, S.R., Wu, M.C., Shih, H.H., Zheng, Q., Yen, N.C., Tung, C.C., and Liu, H.H. (1998). The empirical mode decomposition and the hilbert spectrum for nonlinear and non-stationary time series analysis. In *Proceedings of the Royal Society of London A: mathematical, physical and engineering sciences*, volume 454, 903–995. The Royal Society.

Jiang, H., Choudhury, M.S., and Shah, S.L. (2007). Detection and diagnosis of plant-wide oscillations from industrial data using the spectral envelope method. *Journal of Process Control*, 17(2), 143–155.

Lang, X., Zhang, Z., Xie, L., Horch, A., and Su, H. (2018). Time-frequency analysis of plant-wide oscillations using multivariate intrinsic time-scale decomposition. *Industrial & Engineering Chemistry Research*, 57(3), 954–966.

Mandic, D.P., ur Rehman, N., Wu, Z., and Huang, N.E. (2013). Empirical mode decomposition-based time-frequency analysis of multivariate signals: The power of adaptive data analysis. *IEEE signal processing magazine*, 30(6), 74–86.

Niederreiter, H. (1992). *Random number generation and quasi-Monte Carlo methods*. SIAM.

Rehman, N. and Mandic, D.P. (2009). Multivariate empirical mode decomposition. In *Proceedings of The Royal Society of London A: Mathematical, Physical and Engineering Sciences*, rspa20090502. The Royal Society.

Tangirala, A.K., Shah, S.L., and Thornhill, N.F. (2005). Pscmap: A new tool for plant-wide oscillation detection. *Journal of Process Control*, 15(8), 931–941.

Thornhill, N.F., Cox, J.W., and Paulonis, M.A. (2003a). Diagnosis of plant-wide oscillation through data-driven analysis and process understanding. *Control Engineering Practice*, 11(12), 1481–1490.

Thornhill, N.F., Huang, B., and Zhang, H. (2003b). Detection of multiple oscillations in control loops. *Journal of Process Control*, 13(1), 91–100.

Thornhill, N.F., Shah, S.L., Huang, B., and Vishnubhotla, A. (2002). Spectral principal component analysis of dynamic process data. *Control Engineering Practice*, 10(8), 833–846.

Wu, L.C., Chen, H.H., Horng, J.T., Lin, C., Huang, N.E., Cheng, Y.C., and Cheng, K.F. (2010). A novel preprocessing method using hilbert huang transform for maldi-tof and seldi-tof mass spectrometry data. *Plos One*, 5(8), e12493.